MR IMAGE ENHANCEMENT: A PDE-BASED APPROACH INTEGRATING A DOUBLE-WELL POTENTIAL FUNCTION FOR THIN STRUCTURE PRESERVATION

A. Histace
ETIS UMR CNRS 8051, ENSEA-UCP, 6 avenue du Ponceau, 95014 Cergy, France
aymeric.histace@ensea.fr

M. Ménard
L3i, University of La Rochelle, Pole Sciences et Technologie, 17000 La Rochelle, France
michel.menard@univ-lr.fr

Keywords: Image Diffusion, Double well potential, Directional diffusion, Selectivity.

Abstract: Non-linear or anisotropic regularization PDE's (Partial Differential Equation) raised a strong interest in the field of medical image processing. The benefit of PDE-based regularization methods lies in the ability to smooth data in a nonlinear way, allowing the preservation of important image features (contours, corners or other discontinuities). In this article, we propose a PDE-based method restoration approach integrating a double-well potential as diffusive function. It is shown that this particular potential leads to a particular regularization PDE which makes the integration of prior knowledge about the gradient intensity level to enhance possible. The corresponding method shows interesting properties regarding stability and preservation of fine structures. As a proof a feasibility, results of restoration are presented on natural images to show potentialities of the proposed method. We also address a particular medical application: enhancement of tagged cardiac MRI.

1 INTRODUCTION

In the particular field of image restoration, non-linear or anisotropic regularization PDE's are of primary interest. The benefit of PDE-based regularization methods lies in their ability to smooth data in a nonlinear way, allowing the preservation of important image features (contours, corners or other discontinuities). In the particular domain of scalar image restoration, a lot of studies have been presented in the literature so far: (Perona and Malik, 1990), (Alvarez et al., 1992), (Catté et al., 1992), (Geman and Reynolds, 1992), (Nitzberg and Shiota, 1992), (Whitaker and Pizer, 1993), (Weickert, 1995), (Deriche and Faugeras, 1996), (Weickert, 1998), (Terebes et al., 2002), (Tshumperlé and Deriche, 2002), (Tschumperle and Deriche, 2005) for the main references.

In the particular field of medical image processing, PDE based approach for denoising are very promising tools, but generally needs to be adapted to the imaging context (PET, CT, Cone-beam CT, MRI, etc.) since noise can be of very different types (Gaussian, Poisson, Rayleigh). In (Histace et al., 2009), we showed that, considering a particular general parameterizable PDE, it was possible to integrate selectivity regarding the gradient directions to diffuse or not within the considered image. Qualitative and quantitative results were also presented on a particular medical application: enhancement of tagged cardiac MRI.

In this article, we propose a complementary PDE to the one presented in (Histace et al., 2009) which enables integration of selectivity regarding the intensity of the gradient to restore and which makes the preservation of thin structures from the diffusive effect possible. More precisely, we propose to make this selectivity possible thanks to the integration of a double-well potential diffusion function within the classical Perona-Malik's PDE (Perona and Malik, 1990). That kind of approaches can be of interesting benefits for medical image restoration and particularly for MRI enhancement, since even thin structures can be of primary importance to establish the most appropriate diagnosis.

Our aims and motivation for such a study are mainly to show that, firstly, such a choice can lead to a stable PDE-based approach for scalar image denoising that can overpass classical approach of Perona-

Malik's from which it is derived and which presents instability problems as formerly shown in (Catté et al., 1992). Secondly, we also want to show that this integration leads to a selective PDE-based approach that overcomes classical mean curvature or tensor driven diffusion problems, which in the particular case of directional diffusion are not suitable (see (Histace et al., 2005) and (Terebes et al., 2002)) because they tend to smooth transitions between patterns.

Regarding the medical application we want to address in this article, we propose to tackle a known problem of us: enhancement of tagged cardiac MRI. Such a choice is guided by the fact that we have already worked on that particular MR imaging sequence and that qualitative results have already been computed for comparison. Moreover, as said in section 3, this particular sequence of acquisition can be of primary importance for the follow-up of cardiovascular pathologies and totally fit the problem we want to address: preservation of thin structures within the enhanced data.

This article is organized as follows: In a section two, we propose some recalls about PDE-based regularization approaches. Section three deals with the general presentation of the tagged cardiac MR images problematic. Fourth section is dedicated to the study of the double well function and of its mathematical properties. Prospective results on "lena" are also shown in this section. Section five deals with the enhancement of tagged MRI: Comparative results are shown and commented. Finally, the proposed approach and the obtained results are discussed in last section.

2 PDE based regularization approach: a general scheme

In (Deriche and Faugeras, 1996), authors propose a global scheme for PDE-based restoration approaches. More precisely, if we denote $\psi(\mathbf{r},t) : \mathbb{R}^2 \times \mathbb{R}^+ \rightarrow \mathbb{R}$ the time intensity function of a corrupted image $\psi_0 = \psi(\mathbf{r},0)$, the corresponding regularization problem of ψ_0 is equivalent to the minimization problem described by the following PDE:

$$\frac{\partial \psi}{\partial t} = c_\xi(\|\nabla\psi\|)\frac{\partial^2\psi}{\partial\xi^2} + c_\eta(\|\nabla\psi\|)\frac{\partial^2\psi}{\partial\eta^2} \quad , \quad (1)$$

where $\eta = \nabla\psi/\|\nabla\psi\|$, $\xi \perp \eta$ and c_ξ and c_η are two weighting functions (also called diffusive functions). This PDE can be interpreted as the superposition of two monodimensional heat equations, respectively oriented in the orthogonal direction of the gradient and in the tangential direction: It is characterized by an anisotropic diffusive effect in the privileged directions ξ and η allowing a non-linear denoising of scalar image.

Eq. (1) is of primary importance, for all classical methods can be expressed in that global scheme: For instance, if we consider the former anisotropic diffusive equation of Perona-Malik's (Perona and Malik, 1990) given by

$$\frac{\partial \psi}{\partial t} = div\left(c(\|\nabla\psi\|)\nabla\psi\right) \ , \quad (2)$$

with $\psi(\mathbf{r},0) = \psi_0$ and $c(.)$ a monotonic decreasing function, it is possible to express it in the global scheme of Eq. (1) with

$$\begin{cases} c_\xi = c(\|\nabla\psi\|) \\ c_\eta = c'(\|\nabla\psi\|).|\nabla\psi| + c(\|\nabla\psi\|) \end{cases} \quad (3)$$

Formulation of Eq. (1) is also interesting, for it makes stability study of classical proposed methods possible. More precisely, a stable PDE-based method for denoising will be characterized by a weighting function c_η positive for all values of $\|\nabla\psi\|$ as formerly shown in (Catté et al., 1992). In practice, $c_\eta(.)$ function has also to be of small values in order to diffuse the data in the tangential direction of the image boundaries only.

This last property is of primary importance for the preservation of thin structures since only a "small" diffusive effect in the orthogonal direction of the corresponding gradient can lead to a low alteration of them.

What we proposed in this article is a study for the integration of a double well potential as a diffusive function $c(.)$ in Eq. (2).

3 Tagged cardiac MRI

Mainly, to help cardiologists to establish a pre surgery scheme for reperfusion of myocardial tissue after an infarction, a study of the myocardial local viability is necessary: Whereas classical cardiac MRI does not make the study of the local contraction of the myocardium possible, tagged cardiac MRI allows this local estimation. More precisely, the classical SPAMM (Space Modulation of Magnetization) acquisition protocol (Zerhouni et al., 1988) used for the tagging of MRI data, displays a deformable 45-degrees oriented dark grid which describes the contraction of myocardium (Fig. 1) on the images of temporal Short-Axis (SA) sequences. This is the temporal tracking of this grid that can enable radiologists to evaluate the local intramyocardial displacements.

Figure 1: SA tagged MRI of the Left Ventricle (LV) extracted from a sequence acquired between end-diastole and end-systole.

Tagged cardiac images present peculiar characteristics which make the analysis difficult. More precisely, images are of low contrast compared with classical MRI, the level of corrupting noise is more important than with classical acquisition and their resolution is only of approximately one centimeter. Numerous studies were carried out concerning the analysis of the deformations of the grid of tag on SA sequences (see (Petitjean et al., 2005; Axel et al., 2007) for a complete overview) but all have in common the necessary enhancement of tagged cardiac images which can be considered as thin oriented structures since they are only three or four pixels wide.

Classically, in such a framework (oriented pattern enhancement), the classical Edge Enhancing Diffusion (EED) (Weickert, 1995) normally leads to very satisfying results of regularization. However, as shown in Fig. 10.(c), the poor quality of tagged cardiac images makes the computation of the local structure tensor difficult and, as said in the introduction of this article, that kind of approaches tends to always smooth in the orthogonal direction of the image contours: thin stucture are then altered.

As a consequence, diffusive restoration approaches like the Perona-Malik's former one (Perona and Malik, 1990) are more adapted to our purpose: A non-linear smoothing of the data is performed by taking into consideration the local value of the gradient intensity. If this value is small then the corresponding data are diffused along the tangential direction of the contour. On the contrary, if this value is important the diffusive effect is stopped. That kind of approaches makes the enhancement of the boundaries of the image possible. Nevertheless, as one can notice on Fig. 2, due to the fact that norms of the gradient levels of tagged MRI are very noisy, it is necessary to develop a method that integrates within diffusion process more than only this classical parameter: for instance, calculation and integration of the direction of local gradients of the grid could be of primary interest.

This can be achieved by considering some variations of the classical restoration approaches. We propose for example to consider a variant of the Perona-Malik's process (Perona and Malik, 1990) given by

$$\frac{\partial \psi}{\partial t} = div(c(||\mathbf{A}.\nabla\psi||)\nabla\psi) \; . \tag{4}$$

with $c(u) = e^{-\frac{u^2}{k^2}}$ (as proposed by Perona and Malik) and $\mathbf{A}$ is a vector field defining the particular direction(s) to preserve from the diffusion process (in this particular medical application, the gradient direction of the grid). k represents here a soft threshold driving the decrease of $c(.)$. In both cases, the directional weighting of the diffusion process is driven by the scalar product between the norm of the local gradient and $\mathbf{A}$. As a consequence when local gradient and $\mathbf{A}$ are parallel, there is no diffusion, for $c(||\mathbf{A}.\nabla\psi||) = 0$, whereas all other directions are diffused: the grid of tags is normally enhanced.

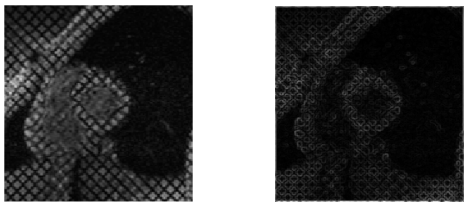

(a) (b)

Figure 2: (a) Original Image, (b) Norm of the corresponding gradients.

Nevertheless, because of instability problems (see section 4 for more details) of PM's approach, it appears that process of Eq. (4) does not lead to interesting results (see Fig. 10.(b)). Such a problem can be overcome by a Gaussian filtering of the gradient data as proposed in (Catté et al., 1992). But, such a Gaussian filtering will also have for consequences an increase of the values corresponding to the diffusive effect in the orthogonal direction of the contours. As explained before, the corresponding approach will then not make preservation of thin structures possible.

Moreover, the classical $c(.)$ function does not allow to integrate within the iterative restoration scheme selectivity regarding the preservation of particular gradient levels. However, such a selectivity would be of significant benefits since value of the tags' gradient can be easily identified (Denney, 1999).

To overpass the drawbacks of Eq. (4) , we propose to dethin $c(.)$ as a double well potential function. This particular function will make integration of gradient level selectivity possible as well as the obtaining of a stable PDE and the preservation of thin structures.

4 Double well potential and corresponding PDE

4.1 Diffusive function

The double well potential considered in this article is dethind by the following function:

$$\phi(u) = \int_0^u v(\alpha - v)(v-1)dv \; . \tag{5}$$

Some graphical representations of Eq. (5) for different values of α are proposed Fig. 3.(a). The roots of the corresponding non linear force (i.e. $f(u) = u(\alpha-u)(u-1)$) 0, and 1 corresponds to the local positions of the minima of the potential, whereas the root α represents the position of the potential maximum. The non linearity threshold α dethins the potential barrier between the potential minimum with the highest energy and the potential maximum.

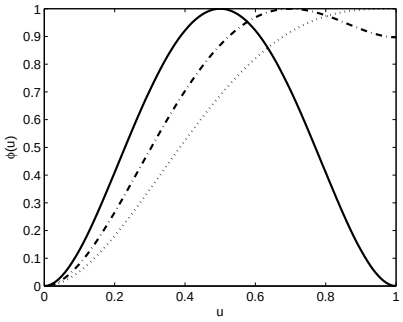

Figure 3: plots of double well potential $\phi(.)$ of Eq. (5) for different values of $\alpha \in [0.5, 1]$. Solid lines stand for $\alpha = 0.5$, dash-dotted lines for $\alpha = 0.7$ and dotted lines for $\alpha = 1$.

This function has to be compared with the classical Perona-Malik's function $c_{PM}(.)$ given by:

$$c_{PM}(u) = e^{-\frac{u^2}{k^2}} \; , \tag{6}$$

with k a soft threshold defining selectivity of $c_{PM}(.)$ regarding values of image gradients. Fig. 4 shows graphical representations of $c_{PM}(.)$ dethind by Eq. (6) for different values of k.

As one can notice on Fig. 4.(a), for $\|\nabla\psi\| \rightarrow 0$, $c_{PM}(\|\nabla\psi\|) \rightarrow 1$, whereas for $\|\nabla\psi\| \rightarrow 1$, $c_{PM}(\|\nabla\psi\|) \rightarrow 0$. As a consequence, boundaries within images which are on a threshold, function of k, are preserved from the smoothing effect of Eq. (2). Regarding Fig. 3, in order to preserve this major property with integration of Eq. (5) as a diffusive function in Eq. (2), it is necessary to dethin this diffusive function as follows:

$$c_{DW}(u) = 1 - \phi(u) \; . \tag{7}$$

Graphical representations of c_{DW} are proposed in Fig. 5.

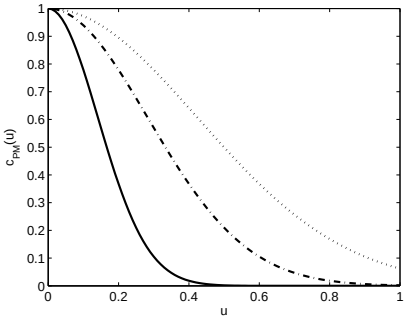

Figure 4: Plots of function $c_{PM}(.)$ of Eq. (6) for different values of k. Solid lines stand for $k = 0.2$, dash-dotted lines for $k = 0.4$, and dotted lines for $k = 0.6$.

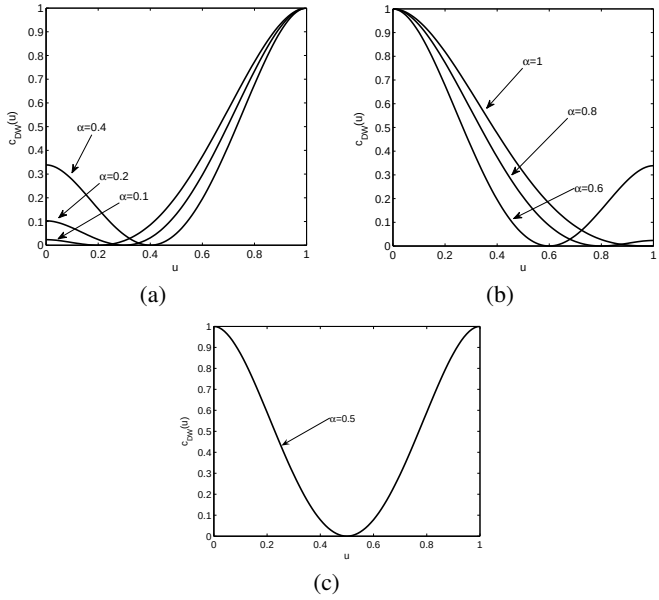

Figure 5: Plots of function $c_{DW}(.)$ of Eq. (5) for different values of α: (a) $0 < \alpha < 0.5$, (b) $0.5 < \alpha < 1$, and (c) $\alpha = 0.5$.

One can notice on Fig. 3 that $\phi(.)$ has been normalized. As a consequence, we are able to ensure that $0 \leq c_{DW}(u) \leq 1$ for all values of u like classical PM's function of Eq. (2). For $0 \leq \alpha < 1$, since c_{DW} is issued from a double well potential, selectivity of Eq. (2) is more important and centered on a particular gradient value function of α. For instance, for $\alpha = 0.5$, only gradients of value 0.5 are totally preserved from the

diffusive effect in the tangential direction. This can be interpreted as an integration of gradient level selectivity within the restoration process.

Moreover, we are now going to show, that integration of c_{DW} as diffusive function leads to interesting stability property of corresponding PDE regarding properties of the corresponding c_η function.

4.2 Study of stability

It is recognized that classical Perona-Malik's PDE presents instability problems. More precisely, as shown in (Catté et al., 1992), sometimes noise can be enhanced instead of being removed. This can be explained considering Eq. (3). If we consider $c_{PM}(.)$ function of Eq. (6), it appears that corresponding $c_{\eta_{PM}}$ function of Eq. (3), in the global scheme of Eq. (1), can sometimes takes negative values (see Fig. 6 for illustrations). This leads to local instabilities of the Perona-Malik's PDE which degrades the processed image instead of denoising it.

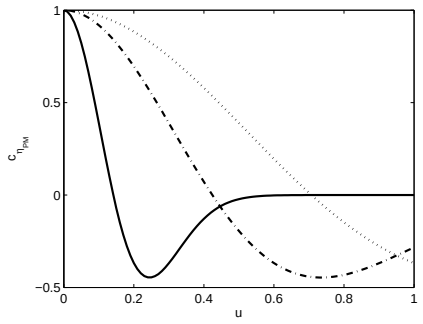

Figure 6: Plots of function $c_{\eta_{PM}}$ for different values of k . Solid lines stand for $k = 0.2$, dash-dotted lines for $k = 0.4$ and dotted lines for $k = 0.6$.

Now, if we calculate mathematical expression of c_η with $c(.) = c_{DW}(.)$ of Eq. (7), one can obtain that:

$$c_{\eta_{DW}}(\|\nabla\psi\|) = c'_{DW}(\|\nabla\psi\|).|\nabla\psi| + c_{DW}(\|\nabla\psi\|) \,, \tag{8}$$

Taking into account that $|\nabla\psi| \in [0..1]$ and that $c'_{DW}(\|\nabla\psi\|)$ is a one-order-less polynomial function than $c_{DW}(\|\nabla\psi\|)$, it happens that:

$$c_{\eta_{DW}}(\|\nabla\psi\|) \approx c_{DW}(\|\nabla\psi\|) = c_\xi(\|\nabla\psi\|) \,. \tag{9}$$

Considering Eq. (9), one can notice that corresponding c_η function never takes negative values (see Fig. 5 for illustrations): Diffusive process remains stable for all gradient values of processed image which is of primary importance.

Moreover, we can also notice that $c_{\eta_{DW}}$ is exactly equal to 0 when $c_{\xi_{DW}} = 0$. As a consequence, by a judicious choice of α, it becomes possible to completely stop the diffusion process in the tangential and orthogonal directions of the contours at the same time. thin structures characterized by an identified gradient level can be preserved from any alterations.

4.3 Experimental results

We propose in this section to make a visual and quantitative comparison between classical Perona-Malik's PDE of Eq. (2) with diffusive function $c(.) = c_{PM}(.)$ of Eq. (6), and the following PDE given by:

$$\frac{\partial\psi}{\partial t} = div\left(c_{DW}(\|\nabla\psi\|)\nabla\psi\right) \,. \tag{10}$$

For practical numerical implementations, the process of Eqs. (2) and (10) are sampled with a time step τ. The restored images $\psi(t_n)$ are calculated at discrete instant $t_n = n\tau$ with n the number of iterations.

We propose to compare our proposed method with PM's approach on the classical "lena" image. For our purpose, this latter has been corrupted by a white Gaussian noise of mean zero and standard deviation σ (see Fig. 7).

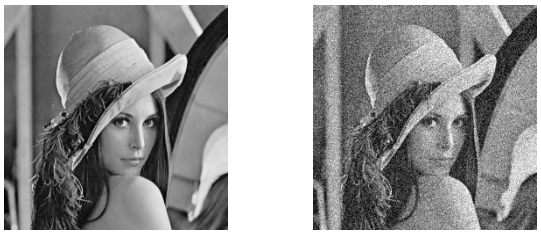

(a) (b)

Figure 7: (a) Original image "lena" and (b) its corrupted version ψ_0 . Corrupting noise is a white Gaussian one of mean zero and standard deviation $\sigma = 0.1$.

Considering nature of non corrupted image (Fig. 7.(a)), quantification of the denoising effect of Eq. (2) with $c(.) = c_{PM}(.)$ and $c(.) = c_{DW}(.)$, will be estimated with a classical PSNR measurement.

Once again, because aim of this article is to show potentiality of the described restoration method, only optimal results for both compared approaches are presented Figs. 8 and 9.

One can notice on Figs. 8 and 9 that both visually and quantitatively, it is possible to find a value of α that can outperform results of optimal classical PM's

(a)

(b)

Figure 8: (a) Restored image with $c(.) = c_{PM}(.)$ (classical Perona-Malik's approach), (b) Restored image with $c(.) = c_{DW}(.)$ (proposed approach). The red circles highlight some regions of interest where the preservation of edges are better than with Perona-Malik's approach. k is equal to 1 for PM's restoration approach, α is equal to 0.2 for the proposed approach (Eq. (10) (these values have been empirically tuned). Time step $\tau = 0.05$

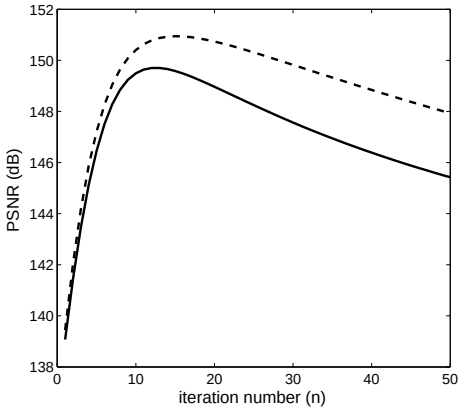

Figure 9: PSNR function of iteration number n, solid lines stands for classical Perona-Malik's approach, dotted line stands for the proposed method (Eq. (10). k is equal to 1, α is equal to 0.2 (these values have been empirically tuned to obtained the best denoising effects). Time parameter $\tau = 0.05$ These two curves have been computed by calculation of the mean results obtained for one hundred different realizations of the Gaussian corrupting noise.

approach. Although the number of iterations corresponding to the optimal restoration results is more important with the proposed approach of Eq. (10) than with PM's approach, quantitatively speaking PSNR is around 2dB higher, and visually speaking, boundaries on Fig. 8.(b) are preserved in a better way from the diffusion effect (see red circles on Fig. 8 for particular regions of interest).

Nevertheless, this example do not permit to directly appreciate the possible gradient level selectivity of the proposed approach. To show it, we are now going to present some results dedicated to the targeted medical application : enhancement of tagged cardiac MRI.

5 Tagged MRI enhancement

We now focus this study on tagged cardiac MRI enhancement.

What we propose here is to compare enhancement results obtained with: (a) the classical PM's approach, (b) the classical Weickert's approach (Weickert, 1995) (Edge Enhancing Diffusion-EED), (c) with PM's approach integrating $c_{DW}(.)$ function (Eq. (10), and (d) with the following PDE:

$$\frac{\partial \psi}{\partial t} = div(c_{DW}(||\mathbf{A}.\nabla\psi||)\nabla\psi) \; . \qquad (11)$$

c_{DW} function is set in order to entirely preserve the gradient level of the tag from diffusion. To achieve this, Fig. 2.(b) is processed so that gradient of the tags are set to 0.5 and the parameter α is set to the same value. This choice made for α is based on the fact that for this particular value, we have shown that the diffusion process is totally stop in both tangential and orthogonal direction of the contours, and is the most selective.

To obtain restoration results with Eq. (11) only one direction of the grid has been taken into account thanks a judicious computation of $\mathbf{A}$. More precisely, each local a priori direction of the corresponding gradient has been estimated thanks to a frequential analysis of processed image (see (Histace et al., 2009) for full detailed of the method). In order to compute a precise estimation of $\mathbf{A}$ from the frequential analysis, we propose to directly use the method of Rao (Rao and Jain, 1992) and Terebes (Terebes et al., 2002). As a consequence, each a priori gradient direction computed from the frequential analysis is preserved from diffusion effect thanks to $\mathbf{A}$, and $c_{DW}(.)$ function makes the enhancement of the tag possible by preserving the gradient level of tags from diffusion.

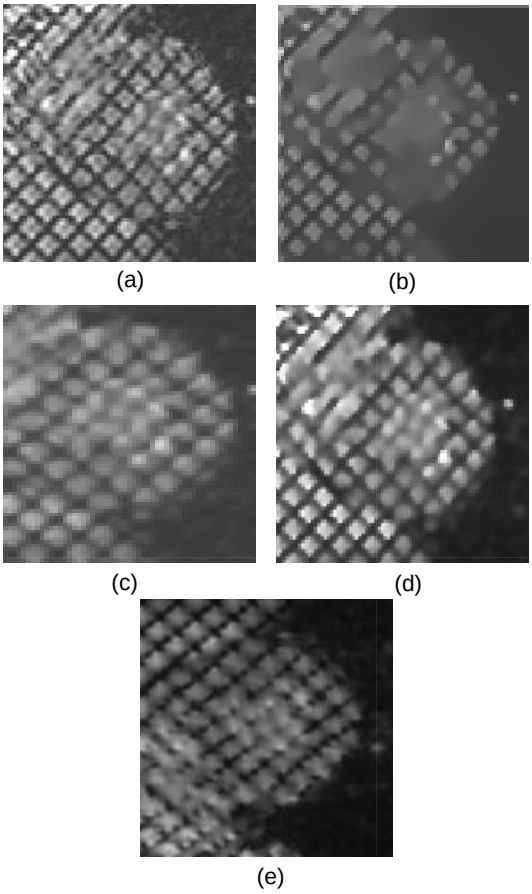

Figure 10: Tagged MRI restoration: (a) Original image, (b) PM's approach, (c) Weickert's approach, (d) PM's approach with $c(.) = c_{DW}(.)$, (e) Result obtained with Eq. (11). "Optimal" visual results for each methods are shown.

As one can notice, the grid enhancement performed thanks to the classical PM's approach (Fig. 10.(b)) presents strong instabilities. As a consequence, the resulting enhanced grid is corrupted and presents no real interest for the tracking of the grid. Considering now the classical Weickert's EED (Fig. 10.(c), one can clearly notice that the method fails in enhancing the tag pattern for the reasons we mentioned earlier in the paper. Fig. 10.(d) shows results obtained with classical PM's approach but with $c(.) = c_{DW}(.)$. The first consequence of such a choice for $c(.)$ function is the absence of stability problems within the iterative enhancing resulting process. As one can see, visually speaking the grid is enhanced and the corresponding boundaries are preserved from the diffusion effect. Moreover, compare to Weickert's EED approach, thin structures (tags mainly) are better preserved. If such a result is of real interest, enhancement effect can be outperformed by considering Eq. (11). This time, result shown Fig. 10.(e) clearly demonstrates the possibility of enhancing the tag patterns by selecting (i) a particular direction, locally computed thanks to a frequential analysis, and (ii) a particular gradient-level characterizing the boundaries of the tags.

6 Discussion and conclusion

In this article, we have proposed an alternative diffusive function for restoration of scalar images within the framework of PDE-based restoration approaches. The proposed diffusive function allows integrating prior knowledge on the gradient level to restore thanks parameter α of Eq. (7) and remains always stable on the contrary of classical PM's approach. Proposed method also remains fast and easy to compute. Visually and quantitatively speaking, better restoration results have been obtained, but this point must be now discussed. Since α parameter finally corresponds to integration of prior information about gradient level to preserve from the diffusion process, it would be interesting to make an adaptive local use of the proposed approach more than a global use.

If interesting visual and quantitative results have been obtained on "lena" image thanks to a global use of the proposed PDE (Eq. (10)), we have also shown that a judicious tuning of this parameter in terms of particular localization within the processed image (Eq. (11) could lead to more interesting results than classical approaches on a particular medical application: enhancement of tagged cardiac MR images. More precisely, thin structures are less altered by the proposed diffusive scheme. Strategy for a local tuning of α still to be now completely automatized. For instance, in the framework of tagged cardiac MRI, it could be of primary interest for the method to be able to adapt the value of α to the fading of the tags due to the non persistency of the magnetization corresponding to the grid (see Fig. 1). More precisely, the fact that this fading phenomenon can be analytically studied would permit such an adaptive setting of α. Moreover, if in this example we choose to select the gradient-level, one could also think about integrating a selectivity upon the grey-level to diffuse or not. This can be achieved by considering a variant of Eq. (11) given by

$$\frac{\partial \psi}{\partial t} = c_{DW_1} div(c_{DW_2}(||\mathbf{A}.\nabla\psi||)\nabla\psi) \; . \qquad (12)$$

In this equation, c_{DW_2}, as shown in this article, permits a selectivity regarding gradient-level, and c_{DW_1} could

permit a selectivity in terms of grey-level intensity. Considering the fact that the grey-level intensity of the myocardium is different from the grey-level intensity of the tags, this approach could be a good alternative for enhancement of tagged cardiac MRI, but also for MR images in general.

REFERENCES

Alvarez, L., Guichard, F., Lions, P., and Morel, J. (1992). Image selective smoothing and edge detection by nonlinear diffusion (ii). *Arch. Rationnal Mech. Anal.*, 29(3):845–866.

Axel, L., Chung, S., and Chen, T. (2007). Tagged mri analysis using gabor filters. In *Biomedical Imaging: From Nano to Macro, 2007. ISBI 2007. 4th IEEE International Symposium on*, pages 684–687.

Catté, F., Coll, T., Lions, P., and Morel, J. (1992). Image selective smoothing and edge detection by nonlinear diffusion. *SIAM Journal of Applied Mathematics*, 29(1):182–193.

Denney, T. (1999). Estimation and detection of myocardial tags in MR images without user-defined myocardial contours. *IEEE Transactions on Medical Imaging*, 18(4):330–344.

Deriche, R. and Faugeras, O. (1996). Les edp en traitements des images et visions par ordinateur. *Traitement du Signal*, 13(6):551–578.

Geman, S. and Reynolds, G. (1992). Constrained restoration and the recovery of discontinuities. *IEEE Transactions on Pattern Analysis and Machine Intelligence*, 14(3):367–383.

Histace, A., Cavaro-Ménard, C., Courboulay, V., and Ménard, M. (2005). Analysis of tagged cardiac MRI sequences. *Lecture Notes on Computer Science (Proceedings of the 3rd Functional Imaging and Modelling of the Heart (FIMH) Workshop)*, 3504:404–413.

Histace, A., Ménard, M., and Cavaro-Ménard, C. (2009). Selective diffusion for oriented pattern extraction: Application to tagged cardiac mri enhancement. *Pattern Recognition Letters*, 30(15):1356–1365.

Nitzberg, M. and Shiota, T. (1992). Nonlinear image filtering with edge and corner enhancement. *IEEE Transactions on Pattern Analysis and Machine Intelligence*, 14(8):826–833.

Perona, P. and Malik, J. (1990). Scale-space and edge detection using anistropic diffusion. *IEEE Transcations on Pattern Analysis and Machine Intelligence*, 12(7):629–639.

Petitjean, C., Rougon, N., and Cluzel, P. (2005). Assessment of myocardial function: A review of quantification methods and results using tagged MRI. *Journal of Cardiovascular Magnetic Resonance*, 7(2):501–516.

Rao, A. and Jain, R. (1992). Computerized flow field analysis: Oriented texture fields. *Transactions on pattern analysis and machine intelligence*, 14(7).

Terebes, R., Lavialle, O., Baylou, P., and Borda, M. (2002). Mixed anisotropic diffusion. In *Proceedings of the 16th International Conference on Pattern Recognition*, volume 3, pages 1051–4651.

Tschumperle, D. and Deriche, R. (2005). Vector-valued image regularization with pde's: A common framework for different applications. *IEEE Transactions on Pattern Analysis and Machine Intelligence*, 27:506–517.

Tshumperlé, D. and Deriche, R. (2002). Diffusion PDEs on vector-valued images. *Signal Processing Magazine, IEEE*, 19(5):16–25.

Weickert, J. (1995). Multiscale texture enhancement. In *Computer Analysis of Images and Patterns*, pages 230–237.

Weickert, J. (1998). *Anisotropic Diffusion in image processing*. Teubner-Verlag, Stuttgart.

Whitaker, R. and Pizer, S. (1993). A multi-scale approac to nonuniform diffusion. *CVGIP:Image Understanding*, 57(1):99–110.

Zerhouni, E., Parish, D., Rogers, W., Yang, A., and Shapiro, E. (1988). Human heart : tagging with MR imaging - a method for noninvasive assessment of myocardial motion. *Radiology*, 169(1):59–63.